Available online at www.ijournalse.org

Emerging Science Journal

(ISSN: 2610-9182)

Vol. 9, No. 6, December, 2025

Multi-Objective Optimization of Injection Molding Using Taguchi, Fuzzy Methods, and GA

Mehdi Moayyedian [1*], Mohammad Reza Chalak Qazani [2, 3], M. Hedayati-Dezfooli [4], Askhat Mussin [1], Zhanel Bissekenova [5]

[1] *College of Engineering and Technology, American University of the Middle East, Egaila 54200, Kuwait.*

[2] *College of Science and Engineering, James Cook University, Townsville, QLD 4815, Australia.*

[3] *Faculty of Computing and Information Technology (FoCIT), Sohar University, Sohar 311, Oman.*

[4] *Department of Mechanical Engineering, College of Engineering and Technology, University of Doha for Science and Technology, Arab League St, Doha P.O. Box 24449, Qatar.*

[5] *Department of Engineering and Technology, American College of the Middle East, Kuwait.*

Abstract

The objective of this research is to optimize the injection molding process of an automotive window regulator bracket by improving the moldability index while minimizing key defects. To achieve this, a multi-objective framework is developed that combines the Taguchi method with Fuzzy Analytic Hierarchy Process (FAHP) and Fuzzy-TOPSIS. Five critical processing parameters—melt temperature, mold temperature, filling time, holding pressure time, and cooling time—were investigated, with polypropylene as the base material. A Taguchi L25 orthogonal array was employed to reduce the number of experimental trials from 3,125 to just 25, thereby saving resources while maintaining reliability. The evaluation considered warpage, residual stress, and shear stress, which are the most influential defects affecting part performance. Finite Element Analysis (FEA) was incorporated to validate the accuracy of the results, while a hybrid ANFIS-GA predictive model was applied to forecast the moldability index, demonstrating an improvement of about 1% over conventional optimization methods. The optimized settings resulted in minimized warpage (1.8122 mm), residual stress (43.03 MPa), and shear stress (0.08 MPa). The novelty of this work lies in integrating Taguchi with FAHP and Fuzzy-TOPSIS for a single-objective transformation, offering a systematic and efficient approach for multi-objective optimization in injection molding applications.

Keywords:

Injection Molding;
Warpage; Shear Stress;
Residual Stress;
FAHP; TOPSIS;
GA; Taguchi Method.

Article History:

Received:	28	April	2025
Revised:	14	November	2025
Accepted:	20	November	2025
Published:	01	December	2025

1- Introduction

Plastic injection molding (PIM) is a widely used manufacturing method for producing complex plastic parts with high dimensional accuracy and repeatability. By injecting molten thermoplastic material into precision molds, this process supports mass production of components with intricate geometries at low cost [1–4]. However, achieving consistent quality requires careful design of parts and molds, precise control of processing conditions, and appropriate material selection [5, 6]. The quality of molded products is strongly influenced by parameters such as melt temperature, mold temperature, cooling conditions, and holding pressure, all of which can lead to defects if not properly optimized. Extensive research has focused on minimizing warpage, shrinkage, and residual stresses in injection-molded components. Studies have explored simulation-based approaches [7–10], optimization

* **CONTACT**: mehdi.moayyedian@aum.edu.kw

DOI: http://dx.doi.org/10.28991/ESJ-2025-09-06-028

frameworks [11–14], and advanced post-processing strategies [15]. Soft computing methods, including artificial neural networks, fuzzy logic, and hybrid models, have also been applied to improve process parameter prediction and defect reduction [16–18]. The Taguchi method has gained popularity due to its ability to systematically reduce experimental trials while maintaining statistical significance [19–21]. Furthermore, fuzzy-based multi-criteria decision-making techniques, such as FAHP and TOPSIS, have been increasingly employed for balancing multiple quality objectives in injection molding [22, 23].

Recent studies published in 2025 provide further advancements in optimizing injection molding for defect reduction. Predictive modeling using fuzzy logic and pattern search optimization effectively minimized warpage and shrinkage in plastic components [24]. Taguchi design combined with computational software demonstrated reduced warpage in complex injection-molded parts [25]. Real-time monitoring of residual stress in transparent polymer parts using a stress intensity indicator was also developed [26]. Simulation-based optimization approaches have further enhanced dimensional accuracy and minimized defects in high-performance injection-molded parts [27]. These studies reinforce the importance of a hybrid methodology to address multiple defects efficiently.

Despite these advances, gaps remain in simultaneously addressing multiple critical defects—particularly warpage, residual stress, and shear stress—through an integrated optimization framework. Many prior studies have optimized single parameters or relied heavily on simulations without effective experimental reduction strategies. Moreover, while surrogate modeling and AI-based tools show promise, their combined application with robust statistical and fuzzy methods is still limited.

To address these limitations, the present study proposes a hybrid methodology that integrates the Taguchi method, FAHP, and Fuzzy-TOPSIS, supported by finite element analysis and a GA-optimized ANFIS predictive model. The approach reduces the required trials from 3,125 to 25 while effectively evaluating five key processing parameters: melt temperature, mold temperature, filling time, holding pressure time, and cooling time. By consolidating multi-objective optimization into a single moldability index, this work advances defect reduction strategies in injection molding and provides a structured framework for achieving more reliable and efficient process settings.

For clarity, the article is organized as follows: The upcoming part explains the selected materials, key process parameters, and experimental design. This is followed by the description of the hybrid optimization framework that integrates the Taguchi method, FAHP, Fuzzy-TOPSIS, and the ANFIS-GA predictive model. The next part highlights and interprets the main results, focusing on defect minimization and moldability index enhancement. The closing part summarizes the contributions of this research and suggests possible directions for future studies.

2- Material and Methods

This research presents an integrated framework combining different optimization tools to achieve optimal process parameters in IM. The main goal is to determine the most effective configurations that improve moldability. The framework is structured into four sequential stages:

- ***Defining the Problem***: This initial phase identifies three major plastic defects as the core quality indicators in the IM process.
- ***Application of FAHP and Taguchi Method***: In this step, the most significant process parameters are prioritized and assigned weights using FAHP, integrated with the Taguchi method to broaden the scope of possible process configurations.
- ***Utilizing the TOPSIS Method***: This method is applied to calculate individual weights for each quality criterion, enabling the identification of parameter combinations that offer the best moldability.
- ***Evaluation of Results***: The final stage focuses on analyzing simulation outcomes to determine the process configurations that achieve the highest Moldability Index, reflecting optimal quality and performance.

This research proposes a structured approach that leverages advanced optimization techniques to assess multiple objectives and determine the best configuration for achieving an optimal moldability index. This cohesive framework allows researchers and manufacturers to tackle multiple quality-related objectives concurrently, considering essential objectives such as warpage, shear stress, and residual stress, all of which significantly influence the quality of the Window Regulator Bracket.

2-1- Problem Description

Evaluating the presence and extent of both internal and external defects in injection-molded components is essential for determining their overall quality. For the selected injected part, common defects impacting quality include warpage, shear stress, and residual stress as shown in Figure 1.

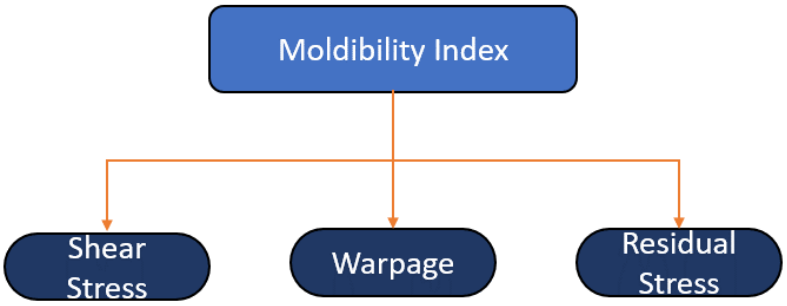

Figure 1. Criteria for quality evaluation

Warpage usually arises during the cooling phase, which follows the initial filling and packing phases. During cooling, the injected molten plastic begins to solidify and shrink, often unevenly, which can cause the part to warp. Shear stress predominantly forms during the filling phase, as the plastic is injected into the cavity at high velocity and pressure. This rapid flow generates friction against the mold walls, resulting in shear stress within the material. Residual stress typically accumulates during the cooling and packing phases. Variations in cooling rates and uneven pressure distribution during packing contribute to internal stresses after it is ejected from the mold.

A fuzzy evaluation approach is used to quantify the severity of each defect in the injection-molded component, classifying them into five distinct levels labeled as $\tilde{\alpha}_1$, $\tilde{\alpha}_2$, $\tilde{\alpha}_3$, $\tilde{\alpha}_4, and\ \tilde{\alpha}_5$. The intensity of defects is defined using linguistic descriptors as shown in Figure 2. To measure defect severity, A membership function is applied, with detailed triplet values provided in Figure 2 and Table 1 [24-26].

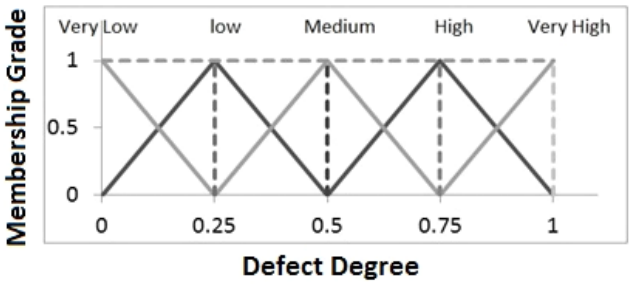

Figure 2. A triangular membership function illustrating the intensity of warpage, shear stress, and residual stress

Table 1. Linguistic variables employed to evaluate the gravity of severity

Linguistic variables	Fuzzy rating	Triple description
Very High	a_5	(0.75, 1, 1)
High	a_4	(0.5, 0.75, 1)
Medium	a_3	(0.25, 0.5, 0.75)
low	a_2	(0, 0.25, 0.5)
Very low	a_1	(0, 0, 0.25)

2-2- Calculation of Importance Values for System Variables

A variable-weight benefit vector is utilized to allocate importance to specific parameters, thereby impacting the assessment of product quality. This method penalizes critical defects by reducing associated negative factors, while minor issues are rewarded by amplifying positive factors. By incorporating tailored adjustment parameters, this approach enables precise regulation of penalty and reward intensity [28-30].

The vector $S(X_j) = \{s_1(x_j), s_2(x_j), \dots, s_p(x_j)\}$ is termed a p-dimensional variable-weight benefit array.

$$(x_j) = \begin{cases} \lambda_1\alpha & x_j = \tilde{\alpha}_1 \\ \alpha & x_j = \tilde{\alpha}_2 \\ 1 & x_j = \tilde{\alpha}_3 \\ \beta & x_j = \tilde{\alpha}_4 \\ \lambda_2\alpha & x_j = \tilde{\alpha}_5 \end{cases} \quad (1)$$

where $j \in \{1,\ 2 \dots, n\}.\alpha, \beta$ and λ the enhancing factor, diminishing and adjustment factors, respectively [30].

2-3- Establishment of Adaptive Weighting

The initial priority values for each objective are established through the Analytic Hierarchy Process (AHP). At the outset, each defect's weight is assigned by assessing the interrelationships between defects and their relative importance. The weight vector W is derived by normalizing the product of a fixed weighting factor *w* and a state vector *s*, as shown in Equation 2 [30].

$$W_j(x_j) = \frac{w_j s_j(x_j)}{\sum_{k=1}^{n} w_k s_k(x_j)} \quad (2)$$

2-4- Taguchi Method and Orthogonal Array

This research adopts an integrative strategy, merging the Taguchi method with various optimization tools to assess moldability indices for injection-molded components. Five process parameters, each set across five distinct levels outlined in Table 2, are chosen based on Fuzzy logic's membership function. Additionally, these parameters are selected due to their prominent influence on the injection process, as evidenced by a comprehensive literature review, to evaluate the defects. The selection of the L25 array is designed with reference to the number of parameters and their levels (see Table 3).

Table 2. Injection Machine parameters and their levels

Parameters	L1	L2	L3	L4	L5
P1: Melt Temp (°C)	200	220	240	260	280
P2: Mold Temp (°C)	20	35	50	65	80
P3: Filling Time (sec)	1	2	3	4	5
P4: Pressure Holding Time (sec)	3	4	5	6	7
P5: Pure Cooling Time (sec)	15	20	25	30	35

Table 3. L25 orthogonal array

Experiment	P_1	P_2	P_3	P_4	P_5
1	1	1	1	1	1
2	1	2	2	2	2
3	1	3	3	3	3
4	1	4	4	4	4
5	1	5	5	5	5
6	2	1	2	3	4
7	2	2	3	4	5
8	2	3	4	5	1
9	2	4	5	1	2
10	2	5	1	2	3
11	3	1	3	5	2
12	3	2	4	1	3
13	3	3	5	2	4
14	3	4	1	3	5
15	3	5	2	4	1
16	4	1	4	2	5
17	4	2	5	3	1
18	4	3	1	4	2
19	4	4	2	5	3
20	4	5	3	1	4
21	5	1	5	4	3
22	5	2	1	5	4
23	5	3	2	1	5
24	5	4	3	2	1
25	5	5	4	3	2

The five selected parameters—melt temperature, mold temperature, filling time, pressure holding time, and pure cooling time—were chosen because prior studies and Fuzzy logic analysis consistently identified them as the most critical factors affecting warpage, shear stress, and residual stress during the filling, packing, and cooling phases. Although other variables such as injection speed or packing pressure may also influence quality, including too many factors would have greatly expanded the design matrix and reduced the practicality of the L25 orthogonal array. The selected set therefore offers a balanced approach, ensuring reliable evaluation of the main defects while keeping the experimental scope manageable. Future work could extend the analysis by integrating additional parameters.

2-5- TOPSIS

This research conducts m experimental trials to assess n specific injection defects for quality evaluation. The process begins by determining the preliminary weights of chosen defects using the AHP. Next, a fuzzy comparison matrix $\tilde{\mathrm{R}} = [\tilde{r}_{ij}]_{m\times n}$ is constructed based on the severity of each potential plastic defect. Using Equations 1 and 2, the unique weight for each criterion is then calculated. Finally, Equation 3 is applied to represent the resultant diversified weighted fuzzy evaluation matrix [30].

$$\tilde{\mathrm{V}} = [\tilde{v}_{ij}]_{m\times n} \quad i = 1, 2, \ldots, m \quad j = 1,2,\ldots,n \tag{3}$$

where;

$$\tilde{v}_{ij} = \tilde{r}_{ij} \times W_j = (r_{ij1}W_j, \quad r_{ij2}W_j, \quad r_{ij3}W_j)$$

The TOPSIS approach is utilized to rank the 25 experiments, with each trial designed to minimize proximity to the positive solution and maximize distance from the negative solution. Then, the elements $\tilde{v}_{ij}$ of normalized positive triangular values are constrained within the interval [0, 1]. Accordingly, the fuzzy positive solution and fuzzy negative solution are defined as shown in Equations 4 and 5 [30]:

$$\mathrm{A}^{+} = \{\tilde{v}_1^{+}\ \tilde{v}_2^{+}\ \ldots\ \tilde{v}_n^{+}\} \tag{4}$$

$$\mathrm{A}^{-} = \{\tilde{v}_1^{-}\ \tilde{v}_2^{-}\ \ldots\ \tilde{v}_n^{-}\} \tag{5}$$

where;

$$\tilde{\mathbf{v}}_{\mathbf{j}}^{+} = \left(v_j^{+}, v_j^{+}, v_j^{+}\right),\ \mathbf{v}_{\mathbf{j}}^{+} = \max\left(v_{ij}^{+}\right), \tilde{\mathbf{v}}_{\mathbf{j}}^{-} = \left(v_j^{-}, v_j^{-}, v_j^{-}\right)\ \&\ \mathbf{v}_{\mathbf{j}}^{-} = \min\left(v_{ij}^{-}\right)$$

The distance calculation for each experiment can be obtained using Equations 6 and 7 [30]:

$$d_i{}^{+} = \sum_{j=1}^{n} d(\tilde{v}_{ij}, \tilde{v}_j{}^{+}), \forall i = 1,2,\ldots,m \tag{6}$$

$$d_i{}^{-} = \sum_{j=1}^{n} d(\tilde{v}_{ij}, \tilde{v}_j{}^{-}), \forall i = 1,2,\ldots,m \tag{7}$$

where $d(\tilde{v}_{ij}, \tilde{v}_j{}^{\pm}) = [1/3((v_{ij1} - v_{11}{}^{\pm})^2 + (v_{ij2} - v_{12}{}^{\pm})^2 + (v_{ij3} - v_{13}{}^{\pm})^2))]^{0.5}$

Finally, the Moldability Index (MI) is calculated as the quality metric for the n options as shown in Equation 8. This index reflects the molding efficiency, shaped by the chosen injection process parameters. A higher MI value indicates improved results with reduced material waste during production [30].

$$MI_i = \frac{d_i{}^{+}}{d_i{}^{+} + d_i{}^{-}}, \quad i = 1,2,\ldots,m. \tag{8}$$

2-6- ANFIS-GA Based Optimization Framework

This study proposes a two-layer optimization methodology that integrates an Adaptive Neuro-Fuzzy Inference System (ANFIS) with a Genetic Algorithm (GA) to further enhance the prediction and optimization of the Moldability Index (MI) in injection molding. While the Taguchi–FAHP–TOPSIS approach efficiently reduced the number of simulations and established a robust decision-making framework, it was limited to the predefined experimental matrix. To overcome this limitation and explore a wider solution space, the proposed framework utilizes machine learning to build a surrogate model capable of predicting MI for untested parameter combinations.

In the first layer, an ANFIS model is constructed using the dataset generated from the 25 simulation trials based on the L25 Taguchi orthogonal array. The five input parameters serve as the input features, and the corresponding MI values calculated from the FAHP-TOPSIS system act as the target output. To enhance the model's accuracy and generalization, GA is applied to optimize the ANFIS hyperparameters, including the number of membership functions, initial step size, and the step size increase/decrease rates. The model performance is evaluated using standard metrics such as root mean square error (RMSE), normalized root mean square error (NRMSE), correlation coefficient (CC), and R^2.

Once the optimal ANFIS model is developed and validated, it is integrated as the fitness function into a second-layer GA optimization loop. In this stage, the Genetic Algorithm explores a larger, continuous input space to identify the optimal combination of input parameters that yield the highest MI. This approach allows for predicting superior configurations beyond the initial L25 trials. The final output of the framework includes both the optimized process parameters and their corresponding predicted MI. To verify the validity of the predicted results, a finite element simulation is performed using the extracted parameters, and the results are compared with those obtained via the conventional Taguchi–FAHP–TOPSIS method.

The hybrid ANFIS-GA framework proposed in this study offers a computationally efficient and accurate solution for multi-objective optimization in IM. It bridges the gap between traditional design-of-experiments-based strategies and intelligent predictive modeling, facilitating informed process optimization with minimal experimental cost.

3- Results and Discussion

The window regulator bracket is a critical component within an automotive window regulator system, enabling the vertical movement of vehicle windows. It serves as a structural support, securing the window glass to the regulator mechanism. Among the materials selected for its fabrication, plastic is widely used due to its versatility and lightweight properties. However, factors such as warpage, shear stress, and residual stress must be carefully addressed during the IM process, as these can significantly impact the structural integrity, surface quality, and overall performance of the component.

As illustrated in Figure 3, a window regulator bracket was precisely designed and selected for simulation analysis using SolidWorks Plastics. Following the modeling phase, a new study was created within SolidWorks Plastics to define the material, configure process parameters, set gate locations, and perform meshing. The injection process employed two designated gates for optimal material flow. To achieve precise results, Finite Element Analysis (FEA) was performed using a solid tetrahedral hybrid mesh, with the size of 4 mm and 3 mm for thicker and thinner sections respectively, resulting in a total of 13,359 solid elements. Polypropylene (P.P) was selected as the material for the injection-molded component, owing to its favorable mechanical and thermal properties.

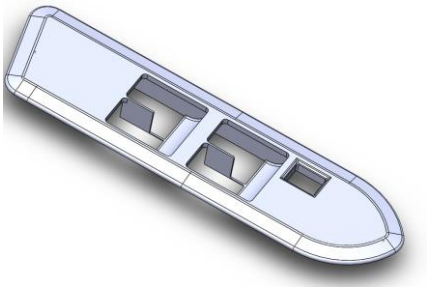

Figure 3. 3D design of window regulator bracket with two gates location

Warpage, shear stress, and residual stress are IM defects that affect part quality. Warpage results from uneven shrinkage during cooling, shear stress arises from molten plastic flow during filling, and residual stress develops due to thermal and pressure imbalances during packing and cooling, impacting dimensional stability and strength [31-33]. SolidWorks Plastics is utilized to thoroughly analyze the identified defects. Using the selected orthogonal array, 25 simulation trials are conducted. Notably, trial 3 demonstrates the lowest warpage, as illustrated in Figure 4.

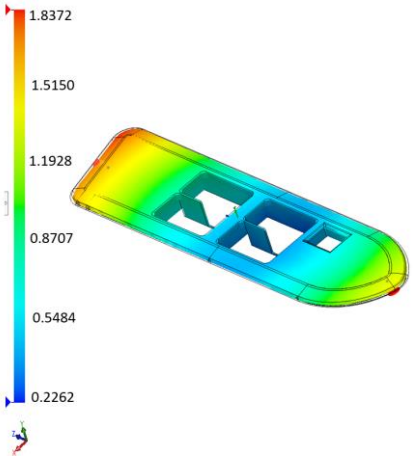

Figure 4. minimum Warpage based on trial 3

Another critical factor examined in this study is shear stress. It arises from the movement of molten plastic through the mold cavity, especially in regions with restricted flow paths or abrupt geometric transitions. High levels of shear stress can result in material degradation, surface imperfections, and weakened areas within the molded component. As shown in Figure 5, trial 15 exhibits the lowest shear stress among the injected components

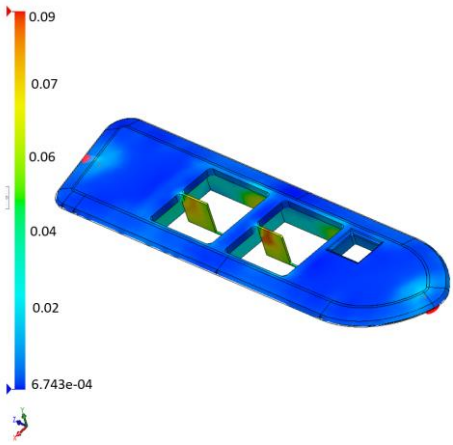

Figure 5. Minimum shear stress based on trial 15

The third critical factor examined in this study is residual stress. Residual stress develops during the packing and cooling stages of the IM process due to uneven temperature distribution and shrinkage. It can result in internal stress within the molded part, leading to warping, dimensional instability, and potential structural weaknesses. As depicted in Figure 6, trial 5 demonstrates the lowest residual stress among the injected components.

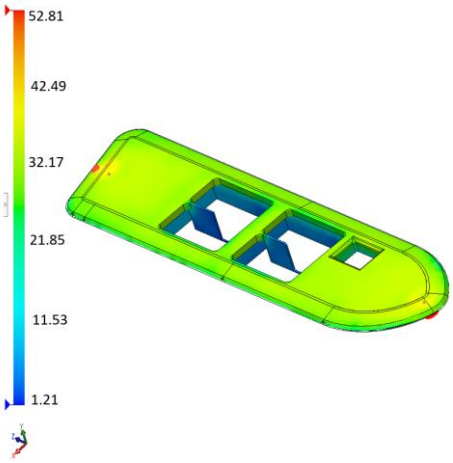

Figure 6. Minimum residual stress based on trial 5

The analysis targets three key plastic defects: warpage, shear stress, and residual stress, with the objective of identifying the trial yielding the lowest defect occurrence in the molded components using SolidWorks Plastics. The initial prioritization and weighting of these defects are established using AHP, as detailed in Table 4, based on the classification framework illustrated in Figure 1.

Table 4. AHP analysis

	S1	S2	S3	Initial weight
Step weight	0.5	0.2	0.3	
Warpage	1			0.5
Shear stress		1		0.3
Residual stress			1	0.2

The evaluation of fuzzy ratings for three specific defects is conducted across 25 trial scenarios. The severity of these defects is quantified using triangular fuzzy numbers, with varying ratings assigned based on their intensity, as outlined in Table 5.

In alignment with expert knowledge, and assuming $\alpha=\beta=1.25$ and $\lambda_1 = \lambda_2 = 1.5$, the weights for each defect are calculated, as presented in Table 6, using Equations 1 and 2. Subsequently, fuzzy logic is applied to evaluate the results of the 25 trials across three distinct defects, as shown in Table 7, in accordance with the methodology outlined in Equation 3.

Table 5. Fuzzy ratings for three types of plastic defects

Trial number	Warpage	Shear stress	Residual stress
1	$\tilde{\alpha}_4$ (0.5,0.75,1)	$\tilde{\alpha}_5$ (0.75,1,1)	$\tilde{\alpha}_2$ (0,0.25,0.5)
2	$\tilde{\alpha}_1$ (0,0,0.25)	$\tilde{\alpha}_4$ (0.5,0.75,1)	$\tilde{\alpha}_2$ (0,0.25,0.5)
3	$\tilde{\alpha}_1$ (0,0,0.25)	$\tilde{\alpha}_3$ (0.25,0.5,0.75)	$\tilde{\alpha}_2$ (0,0.25,0.5)
4	$\tilde{\alpha}_4$ (0.5,0.75,1)	$\tilde{\alpha}_2$ (0,0.25,0.5)	$\tilde{\alpha}_2$ (0,0.25,0.5)
5	$\tilde{\alpha}_1$ (0,0,0.25))	$\tilde{\alpha}_1$ (0,0,0.25))	$\tilde{\alpha}_2$ (0,0.25,0.5)
6	$\tilde{\alpha}_4$ (0.5,0.75,1)	$\tilde{\alpha}_4$ (0.5,0.75,1)	$\tilde{\alpha}_3$ (0.25,0.5,0.75)
7	$\tilde{\alpha}_4$ (0.5,0.75,1)	$\tilde{\alpha}_4$ (0.5,0.75,1)	$\tilde{\alpha}_4$ (0.5,0.75,1)
8	$\tilde{\alpha}_4$ (0.5,0.75,1)	$\tilde{\alpha}_3$ (0.25,0.5,0.75)	$\tilde{\alpha}_2$ (0,0.25,0.5)
9	$\tilde{\alpha}_4$ (0.5,0.75,1)	$\tilde{\alpha}_2$ (0,0.25,0.5)	$\tilde{\alpha}_2$ (0,0.25,0.5)
10	$\tilde{\alpha}_4$ (0.5,0.75,1)	$\tilde{\alpha}_1$ (0,0,0.25)	$\tilde{\alpha}_2$ (0,0.25,0.5)
11	$\tilde{\alpha}_4$ (0.5,0.75,1)	$\tilde{\alpha}_5$ (0.75,1,1)	$\tilde{\alpha}_3$ (0.25,0.5,0.75)
12	$\tilde{\alpha}_5$ (0.75,1,1)	$\tilde{\alpha}_5$ (0.75,1,1)	$\tilde{\alpha}_4$ (0.5,0.75,1)
13	$\tilde{\alpha}_4$ (0.5,0.75,1)	$\tilde{\alpha}_3$ (0.25,0.5,0.75)	$\tilde{\alpha}_4$ (0.5,0.75,1)
14	$\tilde{\alpha}_4$ (0.5,0.75,1)	$\tilde{\alpha}_2$ (0,0.25,0.5)	$\tilde{\alpha}_3$ (0.25,0.5,0.75)
15	$\tilde{\alpha}_4$ (0.5,0.75,1)	$\tilde{\alpha}_1$ (0,0,0.25)	$\tilde{\alpha}_2$ (0,0.25,0.5)
16	$\tilde{\alpha}_4$ (0.5,0.75,1)	$\tilde{\alpha}_5$ (0.75,1,1)	$\tilde{\alpha}_5$ (0.75,1,1)
17	$\tilde{\alpha}_4$ (0.5,0.75,1)	$\tilde{\alpha}_4$ (0.5,0.75,1)	$\tilde{\alpha}_3$ (0.25,0.5,0.75)
18	$\tilde{\alpha}_4$ (0.5,0.75,1)	$\tilde{\alpha}_3$ (0.25,0.5,0.75)	$\tilde{\alpha}_3$ (0.25,0.5,0.75)
19	$\tilde{\alpha}_4$ (0.5,0.75,1)	$\tilde{\alpha}_2$ (0,0.25,0.5)	$\tilde{\alpha}_3$ (0.25,0.5,0.75)
20	$\tilde{\alpha}_5$ (0.75,1,1)	$\tilde{\alpha}_1$ (0,0,0.25)	$\tilde{\alpha}_3$ (0.25,0.5,0.75)
21	$\tilde{\alpha}_4$ (0.5,0.75,1)	$\tilde{\alpha}_3$ (0.25,0.5,0.75)	$\tilde{\alpha}_5$ (0.75,1,1)
22	$\tilde{\alpha}_4$ (0.5,0.75,1)	$\tilde{\alpha}_3$ (0.25,0.5,0.75)	$\tilde{\alpha}_5$ (0.75,1,1)
23	$\tilde{\alpha}_5$ (0.75,1,1)	$\tilde{\alpha}_3$ (0.25,0.5,0.75)	$\tilde{\alpha}_5$ (0.75,1,1)
24	$\tilde{\alpha}_5$ (0.75,1,1)	$\tilde{\alpha}_2$ (0,0.25,0.5)	$\tilde{\alpha}_3$ (0.25,0.5,0.75)
25	$\tilde{\alpha}_5$ (0.75,1,1)	$\tilde{\alpha}_1$ (0,0,0.25)	$\tilde{\alpha}_3$ (0.25,0.5,0.75)

Table 6. Calculation of varying weights using the variable weight profit factor

Trial number	Warpage			Shear stress			Residual stress		
	X_j	$S_j(X_j)$	$w_j(X_j)$	X_j	$S_j(X_j)$	$w_j(X_j)$	X_j	$S_j(X_j)$	$w_j(X_j)$
1	$\tilde{\alpha}_4$	1.25	0.455	$\tilde{\alpha}_5$	1.875	0.273	$\tilde{\alpha}_2$	1.25	0.273
2	$\tilde{\alpha}_1$	1.875	0.600	$\tilde{\alpha}_4$	1.25	0.160	$\tilde{\alpha}_2$	1.25	0.240
3	$\tilde{\alpha}_1$	1.875	0.620	$\tilde{\alpha}_3$	1	0.132	$\tilde{\alpha}_2$	1.25	0.248
4	$\tilde{\alpha}_4$	1.25	0.500	$\tilde{\alpha}_2$	1.25	0.200	$\tilde{\alpha}_2$	1.25	0.300
5	$\tilde{\alpha}_1$	1.875	0.556	$\tilde{\alpha}_1$	1.875	0.222	$\tilde{\alpha}_2$	1.25	0.222
6	$\tilde{\alpha}_4$	1.25	0.532	$\tilde{\alpha}_4$	1.25	0.213	$\tilde{\alpha}_3$	1	0.255
7	$\tilde{\alpha}_4$	1.25	0.500	$\tilde{\alpha}_4$	1.25	0.200	$\tilde{\alpha}_4$	1.25	0.300
8	$\tilde{\alpha}_4$	1.25	0.521	$\tilde{\alpha}_3$	1	0.167	$\tilde{\alpha}_2$	1.25	0.313
9	$\tilde{\alpha}_4$	1.25	0.500	$\tilde{\alpha}_2$	1.25	0.200	$\tilde{\alpha}_2$	1.25	0.300
10	$\tilde{\alpha}_4$	1.25	0.455	$\tilde{\alpha}_1$	1.875	0.273	$\tilde{\alpha}_2$	1.25	0.273
11	$\tilde{\alpha}_4$	1.25	0.481	$\tilde{\alpha}_5$	1.875	0.288	$\tilde{\alpha}_3$	1	0.231
12	$\tilde{\alpha}_5$	1.875	0.556	$\tilde{\alpha}_5$	1.875	0.222	$\tilde{\alpha}_4$	1.25	0.222
13	$\tilde{\alpha}_4$	1.25	0.521	$\tilde{\alpha}_3$	1	0.167	$\tilde{\alpha}_4$	1.25	0.313
14	$\tilde{\alpha}_4$	1.25	0.532	$\tilde{\alpha}_2$	1.25	0.213	$\tilde{\alpha}_3$	1	0.255
15	$\tilde{\alpha}_4$	1.25	0.455	$\tilde{\alpha}_1$	1.875	0.273	$\tilde{\alpha}_2$	1.25	0.273
16	$\tilde{\alpha}_4$	1.25	0.400	$\tilde{\alpha}_5$	1.875	0.240	$\tilde{\alpha}_5$	1.875	0.360
17	$\tilde{\alpha}_4$	1.25	0.532	$\tilde{\alpha}_4$	1.25	0.213	$\tilde{\alpha}_4$	1	0.255
18	$\tilde{\alpha}_4$	1.25	0.556	$\tilde{\alpha}_3$	1	0.178	$\tilde{\alpha}_3$	1	0.267
19	$\tilde{\alpha}_4$	1.25	0.532	$\tilde{\alpha}_2$	1.25	0.213	$\tilde{\alpha}_3$	1	0.255
20	$\tilde{\alpha}_5$	1.875	0.581	$\tilde{\alpha}_1$	1.875	0.233	$\tilde{\alpha}_3$	1	0.186
21	$\tilde{\alpha}_4$	1.25	0.450	$\tilde{\alpha}_3$	1	0.144	$\tilde{\alpha}_5$	1.875	0.405
22	$\tilde{\alpha}_4$	1.25	0.450	$\tilde{\alpha}_3$	1	0.144	$\tilde{\alpha}_5$	1.875	0.405
23	$\tilde{\alpha}_5$	1.875	0.551	$\tilde{\alpha}_3$	1	0.118	$\tilde{\alpha}_5$	1.875	0.331
24	$\tilde{\alpha}_5$	1.875	0.630	$\tilde{\alpha}_2$	1.25	0.168	$\tilde{\alpha}_3$	1	0.202
25	$\tilde{\alpha}_5$	1.875	0.581	$\tilde{\alpha}_1$	1.875	0.233	$\tilde{\alpha}_3$	1	0.186

Table 7. Fuzzy assessment of the outcomes from 25 molding schemes via simulation

Trial number	Warpage	Shear stress	Residual stress
1	(0.23, 0.34, 0.45)	(0.13, 0.2, 0.27)	(0, 0.06, 0.13)
2	(0, 0, 0.15)	(0.08, 0.12, 0.16)	(0, 0.06, 0.12)
3	(0, 0, 0.15)	(0.03, 0.06, 0.09)	(0, 0.06, 0.12)
4	(0.25, 0.37, 0.5)	(0, 0.05, 0.1)	(0, 0.07, 0.15)
5	(0, 0, 0.12)	(0, 0, 0.05)	(0, 0.07, 0.15)
6	(0.26, 0.39, 0.53)	(0.10, 0.15, 0.20)	(0.06, 0.12, 0.18)
7	(0.25, 0.37, 0.5)	(0.04, 0.08, 0.12)	(0.15, 0.22, 0.30)
8	(0.26, 0.39, 0.52)	(0, 0, 0.06)	(0, 0.07, 0.15)
9	(0.25, 0.37, 0.5)	(0.21, 0.28, 0.28)	(0, 0.07, 0.15)
10	(0.22, 0.33, 0.45)	(0.16, 0.22, 0.22)	(0, 0.06, 0.13)
11	(0.24, 0.36, 0.48)	(0.04, 0.08, 0.12)	(0.05, 0.11, 0.17)
12	(0.41, 0.55, 0.55)	(0, 0.05, 0.10)	(0.11, 0.16, 0.22)
13	(0.26, 0.39, 0.52)	(0, 0, 0.06)	(0.15, 0.23, 0.31)
14	(0.26, 0.39, 0.53)	(0.18, 0.24, 0.24)	(0.06,0.12, 0.18)
15	(0.22, 0.33, 0.45)	(0.10, 0.15, 0.21)	(0, 0.06, 0.13)
16	(0.20, 0.30, 0.40)	(0.04, 0.08, 0.12)	(0.19, 0.26, 0.26)
17	(0.26, 0.39, 0.53)	(0, 0.05, 0.10)	(0.06, 0.12, 0.18)
18	(0.27, 0.41, 0.55)	(0, 0, 5.70)	(0.06, 0.13, 0.19)
19	(0.26, 0.39, 0.53)	(0, 0.05, 0.10)	(0.06, 0.12, 0.18)
20	(0.43, 0.58, 0.58)	(0, 0, 5.70)	(0.04, 0.09, 0.13)
21	(0.22, 0.33, 0.45)	(0.03, 0.07, 0.10)	(0.30, 0.40, 0.33)
22	(0.22, 0.33, 0.45)	(0.03, 0.07, 0.10)	(0.30,0.40, 0.40)
23	(0.41, 0.55, 0.55)	(0.02, 0.05, 0.08)	(0.24, 0.33, 0.33)
24	(0.47, 0.63, 0.63)	(0, 0.04, 0.08)	(0.05, 0.10, 0.15)
25	(0.43, 0.58, 0.58)	(0, 0, 0.05)	(0.04, 0.09, 0.13)

The moldability index for the 25 trial samples is calculated using Equation 8, with the results presented in Table 8. Consequently, trial number 5 demonstrates the highest MI. Combining the Taguchi method with fuzzy logic and TOPSIS offers a significant benefit by broadening the range of moldability index options. After determining the Moldability Index, the next step involves computing the Signal-to-Noise (S/N) ratio, presented in Table 8. This calculation facilitates the development of the Taguchi response table. The response table, detailed in Table 9, identifies the optimal levels of the selected parameters to minimize defects while maximizing the moldability index.

Table 8. Moldability indices and S/N evaluation

Trial number	d_i^+	d_i^-	$d_i^+ + d_i^-$	MI_i	S/N
1	0.726	0.647	1.373	0.529	-5.533
2	1.111	0.288	1.399	0.794	-2.005
3	1.163	0.237	1.400	0.831	-1.612
4	0.859	0.550	1.409	0.610	-4.299
5	1.100	0.198	1.298	0.848	-1.437
6	0.685	0.710	1.395	0.491	-6.180
7	0.616	0.777	1.393	0.442	-7.089
8	0.814	0.591	1.404	0.579	-4.740
9	0.859	0.550	1.409	0.610	-4.299
10	0.923	0.476	1.399	0.660	-3.611
11	0.629	0.756	1.385	0.454	-6.856
12	0.483	0.883	1.365	0.353	-9.033
13	0.665	0.732	1.396	0.476	-6.447
14	0.788	0.615	1.402	0.562	-5.011
15	0.923	0.476	1.399	0.660	-3.611
16	0.589	0.773	1.362	0.433	-7.280
17	0.685	0.710	1.395	0.491	-6.180
18	0.738	0.660	1.398	0.528	-5.548
19	0.788	0.615	1.402	0.562	-5.011
20	0.830	0.908	1.738	0.475	-6.470
21	0.611	0.771	1.382	0.442	-7.090
22	0.601	0.795	1.396	0.431	-7.320
23	0.493	0.873	1.366	0.361	-8.845
24	0.656	0.742	1.398	0.469	-6.572
25	0.714	0.666	1.381	0.517	-5.725

Table 9. Identification of optimum levels

Levels	P1: Melt Temperature	P2: Mold Temperature	P3: Filling Time	P4: Pressure Holding Time	P5: Pure Cooling Time
L1	**-2.977**	-6.587	-5.404	-6.836	-5.327
L2	-5.183	-6.325	-5.130	-5.182	**-4.886**
L3	-6.191	-5.438	-5.719	**-4.941**	-5.271
L4	-6.097	-5.038	-6.215	-5.527	-6.143
L5	-7.110	**-4.170**	**-5.090**	-5.072	-5.932

After determining the optimal level, conducting a simulation is essential to verify that the defect values are significantly lower than the minimum levels of warpage, shear stress, and residual stress, as illustrated in Figures 4 to 6. As a result, the minimum values for warpage, shear stress, and residual stress at the optimal parameter levels are presented in Figures 7 and 8. The moldability index at the optimal levels is 0.8943, which is higher than the value obtained from the 25 experiments, as referenced in Table 8.

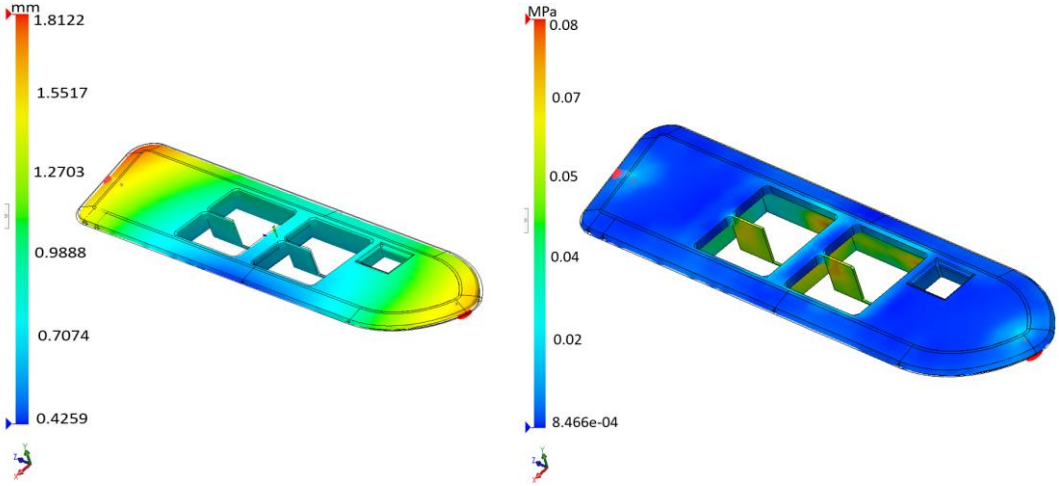

(a) (b)

Figure 7. (a) Optimum Warpage and (b) optimum shear stress

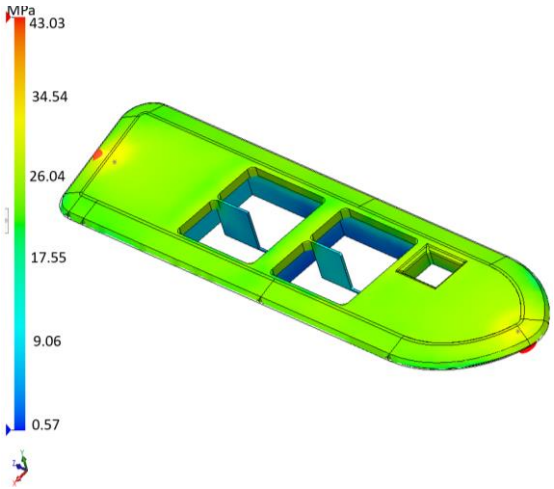

Figure 8. Optimum residual stress

In this work, specific numerical limits for warpage, shear stress, and residual stress were not established, as their acceptable ranges depend strongly on part geometry, thickness, and functional requirements in automotive components. The focus was therefore placed on reducing these defects as much as possible within the experimental design, ensuring that the results remain relevant across a variety of applications where defect minimization is more critical than adhering to a single universal threshold.

The proposed ANFIS model is utilized as the objective function within the Genetic Algorithm (GA) to optimize its hyperparameters, including the initial FIS structure, initial training step size, step size reduction rate, and step size increment rate. Table X1 shows the extracted hyperparameters with other 3 random selection of the hyperparameters.

The comparison presented in Table 10 highlights the superiority of the GA-optimized ANFIS model over randomly selected configurations. The optimized model achieves the lowest RMSE (0.0633) and highest R^2 (0.7060), demonstrating both accuracy and strong generalization capabilities. Notably, the correlation coefficient (CC) remains consistently high across models (≈0.82), but only the optimized setup shows balanced performance across all key metrics, including RMSE and NRMSE.

Table 10. Response Table of Taguchi

Model	Initial FIS	Initial Step Size	Step Size Decrease Rate	Step Size Increase Rate	RMSE	NRMSE	CC	R^2
OPT (GA-based)	2	0.0787	0.2242	1.5973	**0.0633**	**0.1163**	**0.8190**	**0.7060**
Ran1	3	0.0500	0.5000	1.5000	0.2778	0.4266	0.8190	0.4901
Ran2	2	0.1000	0.7500	1.2500	1.5054	2.7657	-0.4606	0.0367
Ran3	3	0.0100	0.2500	1.7500	0.2131	0.3978	0.8206	0.5291

The optimal extracted hyperparameters are used in the generation of our proposed surrogate model to predict the MI of the injection molding process. Figure 9-a illustrates the comparison between actual and predicted Moldability Index (MI) values across the 25 experimental trials. The close alignment between the predicted and observed data points demonstrates the accuracy of the GA-optimized ANFIS model. This visual confirmation supports the performance metrics shown in Table 10, particularly the low RMSE of 0.0633 and high correlation coefficient (CC) of 0.8190.

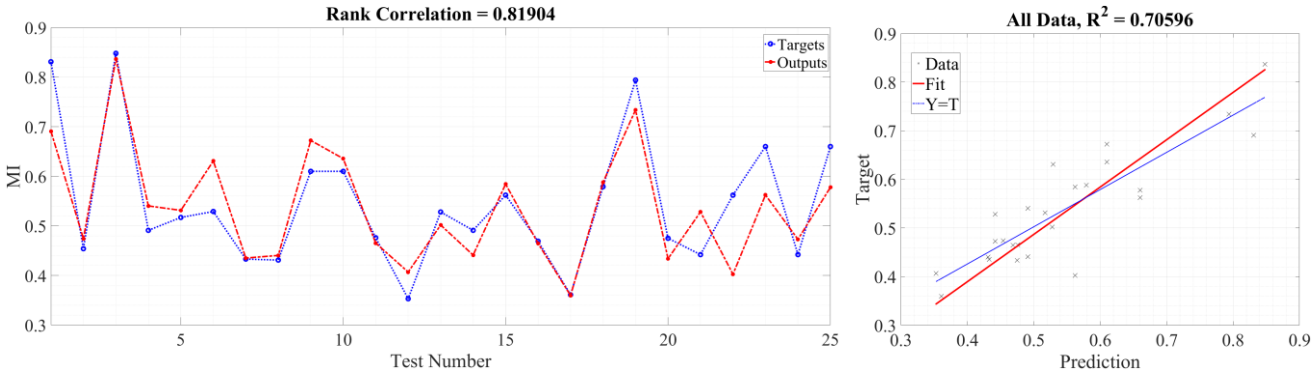

(a) (b)

Figure 9. (a) The actual and predicted MI values across the 25 experimental trials; (b) The regression analysis of the model's predictions

Figure 9-b presents the regression analysis of the model's predictions. The data points closely follow the diagonal reference line, indicating a strong linear relationship between the actual and predicted MI values. This further affirms the model's generalization capability, making it suitable for guiding real-time optimization of IM parameters.

To understand the effect of input parameters on the Moldability Index (MI), three-dimensional response surface plots were generated using the GA-optimized ANFIS model. These plots provide valuable insight into the nonlinear interactions between the process parameters and their impact on MI.

Figure 10-a shows the interaction between Melt Temperature (P1) and Mold Temperature (P2). It was observed that the MI increases significantly as the mold temperature rises from 20°C to 65°C, particularly when the melt temperature is in the range of 220°C to 240°C. The highest MI value of approximately 0.89 occurs when the melt temperature is set to 240°C and the mold temperature is around 65°C. However, when the mold temperature exceeds 70°C, the MI plateaus or slightly decreases. This decline is attributed to excessive thermal exposure, which may lead to delayed solidification or increased warpage. Conversely, at low mold temperatures (20–35°C), the MI remains relatively low regardless of the melt temperature, indicating inadequate mold filling or high residual stress due to poor heat transfer and incomplete packing. These results highlight that a balanced combination of melt and mold temperatures ensures both sufficient material flow and controlled cooling, reducing residual stresses. This trend is consistent with prior studies [7, 25], where excessive mold heating led to unstable shrinkage, whereas moderate heating promoted dimensional stability. Practically, this suggests that industries must avoid pushing mold temperatures too high, even if melt flow improves, since the risk of warpage outweighs the benefits.

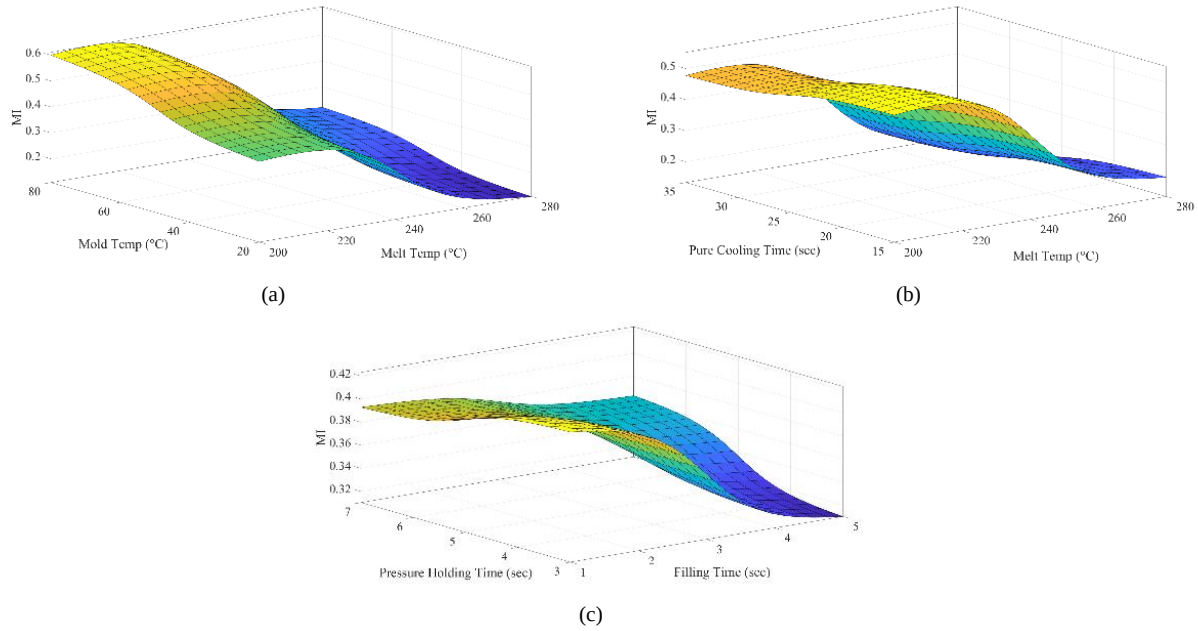

Figure 10. Melt temperature and mold temperature interaction to MI; (b): Melt temperature and pure cooling time interaction to MI; (c): Filling time and pressure holding time interaction to MI

Figure 10-b depicts the interaction between Melt Temperature (P1) and Pure Cooling Time (P5). When the cooling time is less than 20 seconds, the MI remains low (approximately 0.68), particularly when the melt temperature is also low (200–220°C). As the cooling time is extended to 30–35 seconds, the MI rises sharply, surpassing 0.91 when paired with a melt temperature of 240–260°C. Beyond 260°C, increases in melt temperature do not substantially enhance MI, suggesting a saturation point where additional thermal energy no longer contributes positively to molding quality. This behavior underlines the importance of a sufficiently long cooling phase in mitigating warpage and residual stress. The optimal region for MI corresponds to melt temperatures of 240–260°C combined with pure cooling times of 30–35 seconds. This interaction demonstrates that cooling is not merely a secondary step but a dominant factor in final part quality. Insufficient cooling traps thermal gradients, leading to residual stresses, whereas overly long cooling offers diminishing returns and reduces productivity. By identifying the "sweet spot," the framework helps manufacturers strike a balance between cycle time and part quality. Previous optimization studies [12, 28] have also shown that carefully extending cooling significantly lowers internal stresses, supporting our observations.

In Figure 10-c, the effects of Filling Time (P3) and Pressure Holding Time (P4) are illustrated. When both filling time and pressure holding time are short (e.g., 1–2 seconds), the MI is limited, typically ranging between 0.65 and 0.72. As the filling time increases to 4–5 seconds and the pressure holding time reaches approximately 5–6 seconds, the MI improves substantially, reaching values around 0.88 to 0.90. However, further increasing the pressure holding time beyond 6 seconds does not yield significant improvements and may even cause a slight reduction in MI. This suggests that excessive pressure could introduce internal stress or material degradation. The optimum combination for high MI is observed at a filling time of 5 seconds and a pressure holding time between 5 and 6 seconds, where material flow and compaction are adequately balanced. This finding emphasizes the nonlinear role of pressure holding while it ensures cavity packing and reduces voids, excessive pressure exacerbates shear stresses and thermal gradients. Industrially, this means operators must resist the temptation to simply increase pressure for "safety" against voids. Our results align with earlier findings [18, 31] that optimized holding pressure enhances MI, but further increases negative impact stress distribution. This validates the robustness of the proposed model in capturing practical molding trade-offs.

These parametric investigations confirm that the Moldability Index is shaped by the complex, interdependent relationships between process parameters. The optimized ANFIS model can capture these intricate interactions, providing a reliable and computationally efficient tool for predictive analysis and real-time process optimization. The findings support the potential of AI-based surrogate modelling as a powerful complement to traditional simulation-based design and analysis in advanced IM applications.

In the final phase of this study, the GA-optimized ANFIS model was integrated into a Genetic Algorithm (GA) as a fitness function to identify the most effective combination of process parameters for maximizing the Moldability Index (MI). This second-layer optimization enabled an extensive search within the input space, uncovering optimal configurations beyond those tested in the original Taguchi L25 design.

As depicted in Figure 11, the GA converged to a near-optimal solution within approximately 30 generations. The best penalty value reached 99.1541, with a steady decrease in the mean penalty value across generations, indicating improved overall fitness and convergence stability. The optimization yielded the following process parameter

configuration: Melt Temperature (P1 = 211°C), Mold Temperature (P2 = 80°C), Filling Time (P3 = 1 s), Pressure Holding Time (P4 = 3 s), and Pure Cooling Time (P5 = 15 s). These parameters represent a shift toward relatively low melt temperature and very short cycle times compared with the Taguchi–FAHP–TOPSIS results. This suggests that the GA, by exploring a larger solution space, identified an unconventional but effective parameter set that reduces overall thermal exposure while maintaining sufficient compaction. The combination of high mold temperature (80 °C) with very short filling and holding times minimizes cooling gradients and stabilizes shrinkage, explaining the improved MI. Moreover, this solution illustrates the strength of surrogate modeling: the Taguchi-based approach would not have captured this configuration, but the ANFIS–GA framework could. From a practical perspective, this outcome highlights that non-intuitive parameter combinations—such as lower melt temperature with higher mold temperature—can still yield superior part quality if carefully optimized, a point consistent with recent reports on advanced simulation-driven optimization [24–27].

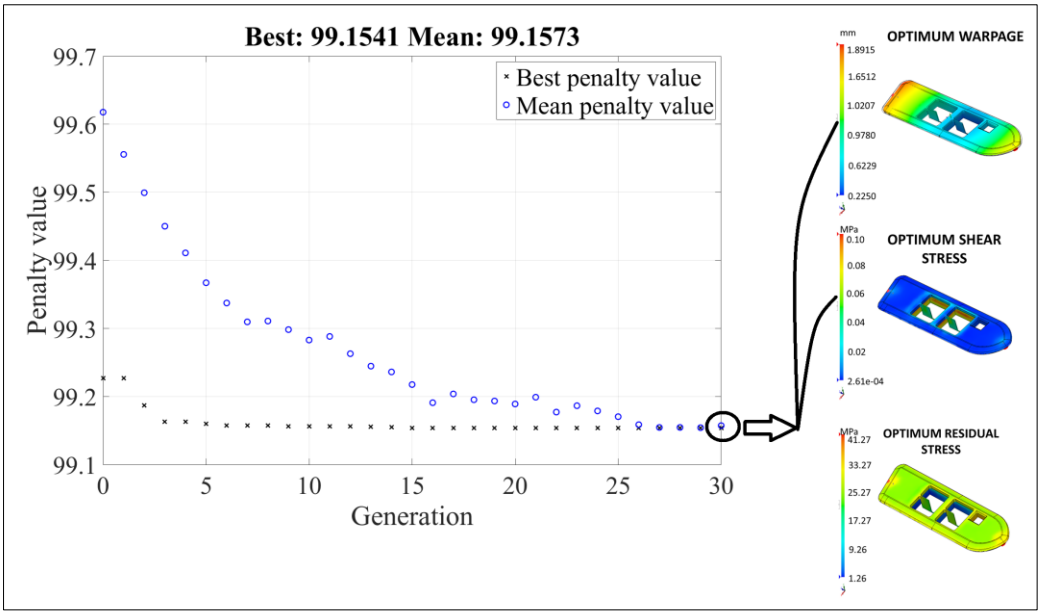

Figure 11. The result of the optimization to reach the minimum defects, including warpage, shear stress, and residual stress

For comparison, Otieno et al. [24] applied fuzzy logic with pattern search optimization to reduce warpage and shrinkage, reporting effective improvements but without integrating residual stress into the evaluation. Zhang et al. [25] combined Taguchi design with Moldflow software, demonstrating significant warpage reduction in complex parts, though their approach did not consolidate multiple defect types into a single optimization framework. Chen et al. [26] focused on real-time residual stress monitoring in transparent polymer parts, offering valuable insights into stress characterization but not providing a multi-objective optimization strategy. Similarly, Tan [27] optimized dimensional accuracy through simulation-based analysis, but the method required extensive computational resources. In contrast, the present study integrates Taguchi, FAHP, Fuzzy-TOPSIS, and ANFIS-GA into a hybrid framework that simultaneously addresses warpage, shear stress, and residual stress. With only 25 initial trials, our model achieved a validated Moldability Index (MI) of 0.8943, representing a ~1% improvement over Taguchi–fuzzy-only methods and offering a more efficient and comprehensive pathway for defect minimization. This comparative analysis demonstrates that the proposed methodology not only aligns with but also extends beyond prior research, providing a robust and generalizable optimization framework for injection molding applications.

To validate this outcome, a finite element simulation was conducted using the extracted parameters. The Moldability Index obtained was 0.8943, which represents a 1% improvement over the best result (MI = 0.884) achieved using the Taguchi–FAHP–TOPSIS method. The right-hand side of Figure 11 illustrates the defect analysis for the optimal configuration: the warpage is minimized to ~1.89 mm, the shear stress is as low as 0.08 MPa, and the residual stress is reduced to ~31.27 MPa. These results confirm that the proposed ANFIS-GA framework effectively generalizes the relationship between parameters and quality metrics, allowing for precise optimization with minimal simulation overhead. The framework is flexible and can be applied to other polymers or geometries by redefining process parameters, defect weightings, and membership functions. Material-specific behavior (e.g., thermal or flow properties) would guide these adjustments. The same optimization and ranking steps can then be repeated to ensure reliable moldability evaluation.

The Moldability Index (MI) was developed as a relative measure, where higher values correspond to improved overall moldability by accounting for reductions in warpage, shear stress, and residual stress. While MI effectively identifies the best processing conditions in this study, it is not an absolute scale and may require normalization or adjustment for practical use in industry, particularly when applied to parts with different geometries, materials, or performance requirements. This ensures that practitioners can interpret the MI consistently and make informed process decisions.

4- Conclusion

The combined use of the Taguchi method, FAHP, and TOPSIS offers a robust framework for multi-objective evaluation and optimal selection in IM, targeting components with the highest moldability index. In this approach, the Taguchi method is used to analyze three prevalent plastic defects across five key process parameters, each examined at five different levels. A fuzzy logic-based evaluation system categorizes defect severity into five levels, with initial weightings derived using AHP. The L25 orthogonal array streamlines the assessment of potential configurations, while TOPSIS is employed to rank these 25 experimental trials based on their overall performance. A detailed numerical analysis considers the impact of all three defects, and the accuracy of the results is further validated through Finite Element Analysis (FEA). The highest moldability index, 0.848, was achieved in trial number 5 from the 25 trials. By combining Taguchi with Fuzzy TOPSIS, the optimum moldability index was determined, with fewer selected defects. The optimal moldability index, 0.8943, demonstrates the effectiveness of the two optimization methods. Additionally, the proposed ANFIS-GA framework demonstrated superior optimization performance by identifying a novel set of input parameters that achieved a validated Moldability Index of 0.8943—1% higher than the best result obtained using traditional methods. Although the proposed method provides a thorough evaluation of quality, its focus is confined to the specific objectives chosen for this study. To enhance its applicability, future research could expand the framework by including a wider range of critical criteria and process parameters in IM, ultimately offering more extensive and versatile guidelines for process optimization. Future work will focus on validating the ANFIS-GA framework with experimental and industrial datasets under noisy conditions, incorporating techniques such as k-fold cross-validation to further assess robustness and generalizability. Also, it could incorporate cross-validation or bootstrapping approaches to further confirm the reliability and generalizability of the ANFIS-GA predictions.

5- Declarations

5-1- Author Contributions

Conceptualization, M.R.Q., M.M., and Z.B.; methodology, M.R.Q. and M.M.; software, M.R.Q., M.M., and Z.B.; validation, M.R.Q.; formal analysis, M.R.Q., M.M., Z.B., and A.M.; investigation, M.M. and M.D.; resources, M.M., M.D., Z.B., and A.M.; data curation, M.R.Q.; writing—original draft preparation, M.R.Q. and A.M.; writing—review and editing, M.R.Q., M.M., and M.D.; visualization, M.D. and A.M.; supervision, M.M.; project administration, M.M. All authors have read and agreed to the published version of the manuscript.

5-2- Data Availability Statement

The data presented in this study are available on request from the corresponding author.

5-3- Funding

The authors received no financial support for the research, authorship, and/or publication of this article.

5-4- Institutional Review Board Statement

Not applicable.

5-5- Informed Consent Statement

Not applicable.

5-6- Conflicts of Interest

The authors declare that there is no conflict of interest regarding the publication of this manuscript. In addition, the ethical issues, including plagiarism, informed consent, misconduct, data fabrication and/or falsification, double publication and/or submission, and redundancies have been completely observed by the authors.

6- References

[1] Min, B. H. (2003). A study on quality monitoring of injection-molded parts. Journal of Materials Processing Technology, 136(1–3), 1–6. doi:10.1016/S0924-0136(02)00445-4.

[2] Moussaoui, H. (2024). Achieving energy savings and process optimization in plastic injection molding: A design of experiments study. Journal of Cleaner Production, 477, 143835. doi:10.1016/j.jclepro.2024.143835.

[3] Kurkin, E., Pioquinto, J. G. Q., Kurkina, E., Pechenik, E., & Chertykovtseva, V. (2024). Heuristic algorithm for the topological optimization of runner system for the thermoplastics injection molding. Journal of Manufacturing Processes, 124, 1393–1409. doi:10.1016/j.jmapro.2024.06.064.

[4] Moayyedian, M., Abhary, K., & Marian, R. (2015). Improved Gate System for Scrap Reduction in Injection Molding Processes. Procedia Manufacturing, 2, 246–250. doi:10.1016/j.promfg.2015.07.043.

[5] Tang, S. H., Kong, Y. M., Sapuan, S. M., Samin, R., & Sulaiman, S. (2006). Design and thermal analysis of plastic injection mould. Journal of Materials Processing Technology, 171(2), 259–267. doi:10.1016/j.jmatprotec.2005.06.075.

[6] Crawford, R. J. (1987). Rubber and plastic engineering design and application. Mechanical Engineering Publications, London, United Kingdom.

[7] Zhao, N., Lian, J., Wang, P., & Xu, Z. (2022). Recent progress in minimizing the warpage and shrinkage deformations by the optimization of process parameters in plastic injection molding: a review. The International Journal of Advanced Manufacturing Technology, 120(1–2), 85–101. doi:10.1007/s00170-022-08859-0.

[8] Lin, M.-Y., Zeng, Y.-J., Hwang, S.-J., Wang, M.-H., Liu, H.-P., & Fang, C.-L. (2022). Warpage and residual stress analyses of post-mold cure process of IC packages. The International Journal of Advanced Manufacturing Technology, 124(3–4), 1017–1039. doi:10.1007/s00170-022-10436-4.

[9] Mukhtarkhanov, M., Shehab, E., & Ali, M. H. (2024). Experimental Study on Warpage Phenomenon of Wax Parts Manufactured by Fused Filament Fabrication. Polymers, 16(2), 208. doi:10.3390/polym16020208.

[10] Wang, J., Liu, T., Zheng, K., Liu, H., Cui, H., & Li, H. (2024). Local thermal warpage deformation of polypropylene injection molded flat part and neural network prediction model. Frontiers in Materials, 11. doi:10.3389/fmats.2024.1421546.

[11] Wang, J., He, J., Li, H., & Fang, K. (2023). Qualitative characterization of residual stress of injection molded polycarbonate goggles based on photoelasticity and digital image processing technique. Frontiers in Materials, 10, 1242721. doi:10.3389/fmats.2023.1242721.

[12] Hiyane-Nashiro, G., Hernández-Hernández, M., Rojas-García, J., Rodriguez-Resendiz, J., & Álvarez-Alvarado, J. M. (2022). Optimization of the Reduction of Shrinkage and Warpage for Plastic Parts in the Injection Molding Process by Extended Adaptive Weighted Summation Method. Polymers, 14(23), 5133. doi:10.3390/polym14235133.

[13] Siabia, A., Sohrabkhani, M., Mahdiani, L. R., & Taghavitabari, A. (2022). The use of Taguchi method in investigation of influence injection molding parameters on the warpage of an industrial component. NeuroQuantology, 20(22), 1845. doi:10.14704/nq.2022.20.22.NQ19638.

[14] Liu, X., Fan, X., Guo, Y., Man, B., & Li, L. (2021). Warpage optimization of the GFRP injection molding process parameters. Microsystem Technologies, 27(12), 4337–4346. doi:10.1007/s00542-021-05241-0.

[15] Sudsawat, S., & Sriseubsai, W. (2018). Warpage reduction through optimized process parameters and annealed process of injection-molded plastic parts. Journal of Mechanical Science and Technology, 32(10), 4787-4799. doi:10.1007/s12206-018-0926-x.

[16] Mohamad Halimin, N. A., Zain, A. M., & Azman, M. F. (2015). Warpage Prediction in Injection Molding Using Artificial Neural Network. Journal of Soft Computing & Decision Support Systems, 2(5), 1-7.

[17] Jacques, M. St. (1982). An analysis of thermal warpage in injection molded flat parts due to unbalanced cooling. Polymer Engineering & Science, 22(4), 241–247. doi:10.1002/pen.760220405.

[18] Leo, V., & Cuvelliez, Ch. (1996). The effect of the packing parameters, gate geometry, and mold elasticity on the final dimensions of a molded part. Polymer Engineering & Science, 36(15), 1961–1971. doi:10.1002/pen.10592.

[19] Tarng, Y. S., & Yang, W. H. (1998). Application of the Taguchi Method to the Optimization of the Submerged Arc Welding Process. Materials and Manufacturing Processes, 13(3), 455–467. doi:10.1080/10426919808935262.

[20] Connor, A. M. (1999). Parameter Sizing for Fluid Power Circuits Using Taguchi Methods. Journal of Engineering Design, 10(4), 377–390. doi:10.1080/095448299261263.

[21] Moayyedian, M., Qazani, M. R. C., & Pourmostaghimi, V. (2022). Optimized injection-molding process for thin-walled polypropylene part using genetic programming and interior point solver. The International Journal of Advanced Manufacturing Technology, 124(1–2), 297–313. doi:10.1007/s00170-022-10551-2.

[22] Kanagalakshmi, S., Manamalli, D., & Rafiq, M. M. (2013). Real time Implementation of multimodel based PID and Fuzzy controller for Injection molding machine. IFAC Proceedings Volumes, 46(32), 493–498. doi:10.3182/20131218-3-in-2045.00037.

[23] Moayyedian, M., Abhary, K., & Marian, R. (2018). Optimization of injection molding process based on fuzzy quality evaluation and Taguchi experimental design. CIRP Journal of Manufacturing Science and Technology, 21, 150–160. doi:10.1016/j.cirpj.2017.12.001.

[24] Otieno, S. O., Wambua, J. M., Mwema, F. M., Mharakurwa, E. T., Jen, T. C., & Akinlabi, E. T. (2025). A predictive modelling strategy for warpage and shrinkage defects in plastic injection molding using fuzzy logic and pattern search optimization. Journal of Intelligent Manufacturing, 36(3), 1835–1859. doi:10.1007/s10845-024-02331-4.

[25] Zhang, L., Chang, T. L., Tsao, C. C., Hsieh, K. C., & Hsu, C. Y. (2025). Analysis and optimization of injection molding process on warpage based on Taguchi design and PSO algorithm. The International Journal of Advanced Manufacturing Technology, 137(1), 981-988. doi:10.1007/s00170-025-15099-5.

[26] Chen, J. Y., Vo, T. P. L., & Huang, M. S. (2025). Real-time monitoring and quantitative analysis of residual stress in thin-walled injection-molded components. Journal of Manufacturing Processes, 141, 991-1001. doi:10.1016/j.jmapro.2025.03.030.

[27] Tan, F. (2025). Simulation-Based Analysis and Optimization of High-Performance Dielectric Strength Polymers in the Injection Molding of Electrical Connectors. Polymers, 17(18), 2465. doi:10.3390/polym17182465.

[28] Guerra, N. B., Reis, T. M., Scopel, T., de Lima, M. S., Figueroa, C. A., & Michels, A. F. (2023). Influence of process parameters and post-molding condition on shrinkage and warpage of injection-molded plastic parts with complex geometry. The International Journal of Advanced Manufacturing Technology, 128(1–2), 479–490. doi:10.1007/s00170-023-11782-7.

[29] He, W., Zhang, Y. F., Lee, K. S., Fuh, J. Y. H., & Nee, A. Y. C. (1998). Automated process parameter resetting for injection moulding: a fuzzy-neuro approach. Journal of Intelligent Manufacturing, 9(1), 17–27. doi:10.1023/a:1008843207417.

[30] Cheng, J., Feng, Y., Tan, J., & Wei, W. (2008). Optimization of injection mold based on fuzzy moldability evaluation. Journal of Materials Processing Technology, 208(1–3), 222–228. doi:10.1016/j.jmatprotec.2007.12.114.

[31] Moayyedian, M., Qazani, M. R. C., Amirkhizi, P. J., Asadi, H., & Hedayati-Dezfooli, M. (2024). Multiple objectives optimization of injection-moulding process for dashboard using soft computing and particle swarm optimization. Scientific Reports, 14(1), 23767. doi:10.1038/s41598-024-62618-7.

[32] Qazani, M. R. C., Moayyedian, M., Amirkhizi, P. J., Hedayati-Dezfooli, M., Abdalmonem, A., Alsmadi, A., & Alam, F. (2024). Multi-Objective Optimisation of Injection Moulding Process for Dashboard Using Genetic Algorithm and Type-2 Fuzzy Neural Network. Processes, 12(6), 1163. doi:10.3390/pr12061163.

[33] Amer, Y., Moayyedian, M., Hajiabolhasani, Z., & Moayyedian, L. (2013). Improving Injection Moulding Processes Using Experimental Design. World Academy of Science, Engineeering and Technology, 75(3), 157–170.